Microelectronics Reliability 150 (2023) 115224

Contents lists available at ScienceDirect

Microelectronics Reliability

journal homepage: www.elsevier.com/locate/microrel

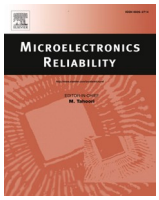

Automated endpointing in microelectronics failure analysis using laser induced breakdown spectroscopy

Pouria Hoveida [1], Adrian Phoulady [1], Hongbin Choi [1], Yara Suleiman, Nicholas May, Toni Moore, Sina Shahbazmohamadi [*], Pouya Tavousi [*]

University of Connecticut, CT, USA

ARTICLE INFO

Keywords:
Laser induced breakdown spectroscopy
Laser-enabled sample preparation and failure analysis
Automation
Laser machining
E
ndpointing

ABSTRACT

Failure analysis of microelectronics is essential to identify the root cause of a device's failure and prevent future failures. This process often requires removing material from the device sample to reach the region of interest, which can be done through various destructive methods, such as mechanical polishing, chemical etching, focused ion beam milling, and laser machining. Among these, laser machining offers a unique combination of speed, precision, and controllability to achieve a high-throughput, highly targeted material removal. In using lasers for processing of microelectronic samples, a much-desired capability is automated endpointing which is crucial for minimizing manual checks and improving the overall process throughput. In this paper, we propose to integrate laser-induced breakdown spectroscopy (LIBS), as a fast and high-precision material detection and process control means, into an ultrashort pulsed laser machining system, to enable vertical endpointing for sample preparation and failure analysis of microelectronics. The capabilities of the proposed system have been demonstrated through several sample processing examples.

1. Introduction

In microelectronics, failure analysis is a critical task for correlating the failure to its root causes, which helps with preventing similar failures from happening in the future. This helps save lives that would be otherwise impacted due to catastrophes and can enhance product yield and reliability, potentially promoting economic viability and profitability. Performing investigations for identification of the defects that have caused a device failure, often requires reaching the region of interest within the device, through removal of material from the device sample. Different destructive methods that can be used for this purpose include mechanical material removal, chemical etching, focused ion beam (FIB) milling [1–3] and laser machining. If used in a controlled fashion, laser can significantly outperform the other alternatives. It offers orders of magnitude higher throughput than FIB, while offering comparable precisions. A comparison of laser with FIB for creating cross-sectional cuts has been provided in [15]. Further, the laser processing is far more controllable and precise than mechanical polishing and chemical etching, while offering comparable throughputs to these methods. In particular, laser scanning enables highly-targeted material removal, which is often not achievable using mechanical and chemical methods. The ability to remove material in a targeted fashion is particularly important for cases that the various components of the device must be preserved as much as possible, for follow-up investigations of other regions or testing the region of interest while the device is powered up [16–20].

Effective use of laser for exposing the region of interest in a targeted fashion requires process control through monitoring. Although process monitoring can be done manually, doing so entails several caveats. First, due to the need for several checks throughout the process, the overall workflow is often extremely slow when high precisions are desired, acting as a prohibitive factor for many throughput-demanding applications. Second, the manual process is prone to human error. Thus, the ability to automate process monitoring and control promises enhancements both in throughput and precision [13,14].

A key aspect of automation, which is particularly imperative for failure analysis of microelectronic samples is automated endpointing in the sample preparation process. Automated endpointing will enable machining to continue until a material region is ended or a certain material region is reached. Such automation capability will minimize

* Corresponding authors.
E-mail addresses: sina.shahbazmohamadi@uconn.edu (S. Shahbazmohamadi), pouya.tavousi@uconn.edu (P. Tavousi).
[1] Co-first authors.

https://doi.org/10.1016/j.microrel.2023.115224
Received 1 June 2023; Received in revised form 26 June 2023; Accepted 25 August 2023
Available online 1 October 2023
0026-2714/© 2023 Published by Elsevier Ltd.

the number of stops that are necessary for conducting manual checks.

To enable endpointing during a laser machining effort, one must either have a 3D map of the composing materials within the sample or must identify the material compositions as the sample undergoes the machining process. The former case requires prior non-destructive, volumetric imaging of the sample and/or having access to the digital design of the sample. It further requires a way to precisely monitor the geometry changes of the sample as it undergoes the lasering process to infer the material composition of the exposed surface at each point in time. The complexities associated with acquiring the 3D compositional map of the sample and constant monitoring of the sample geometry during the laser machining process make the second approach more appealing for most applications. To implement the second approach, namely identification of material composition during the machining process, several different imaging and spectroscopy methods, including energy dispersive X-ray spectroscopy (EDS) and X-ray photoelectron spectroscopy (XPS) [4–6] can be used for investigation of the exposed surface of the sample undergoing the laser processing. However, these methods require the sample to be transferred back and forth between the lasering unit and imaging and spectroscopy devices, which will make the overall process very time consuming and costly. Attempting to perform the measurements less frequently to save on time and cost, will result in compromised precisions.

A technique that promises to address this problem is laser induced breakdown spectroscopy (LIBS), which works based on collecting the signal emitted from the laser-matter interaction plume and analyzing that signal for material detection. Because LIBS can leverage the same laser beam that is used for machining, also for material detection, it negates the need for transferring the sample between the lasering environment and the imaging/spectroscopy instruments. Use of LIBS for material detection and process control has been used in multiple studies for various applications [9–12]. In this paper, we propose to integrate LIBS into an intelligent laser machining system to enable vertical endpointing for sample preparation and failure analysis of microelectronics. Through several examples, the capability of the proposed solution for high-precision endpointing has been showcased.

2. Materials and methods

2.1. Integrated system overview

Fig. 1 provides an overview schematic for the proposed integrated system.

Upon interaction of laser with matter, a laser plume is generated, resulting in a LIBS signal. The signal is collected by the LIBS optics and read by the spectroscope. The read signal is sent in real time to a computer system that rapidly processes the signal for follow-up decision-making about the remainder of the lasering process. The feedback is constantly fed to the lasering system for continuous process control.

2.2. Laser machining system

The laser machining system used in this study features a Coherent Monaco 1035 nm 40 W laser sources (1035-40-40) with a pulse width of 257 fs, capable of producing various pulse repetition rates ranging from single shots to 50 MHz. The laser emits a beam with a diameter of 2.7 ± 0.3 mm, which is expanded using a beam expander made up of a fused silica 75 mm aspherical lens and a fused silica 300 mm convex lens, resulting in a beam diameter of approximately 11 mm. The expanded beam is then directed to a telecentric fused silica F-Theta lens (TSL-1064-10-56Q-D20) with an effective focal length of 70 mm, resulting in a theoretical spot size of around 8.5 μm. Fig. 2 provides a computer-aided design (CAD) illustration of the laser setup used in the study.

The femtosecond machining system workflow begins by targeting the region of interest (ROI) with a Dinolite digital microscope (AM73915MZT) and moving the sample accurately on an XY plane using Zaber LDA series stages (LDA150A-AE53T10A). Next, the Keyence confocal height sensor (CL-P070) measures the sample's height with low micrometer resolution, after which the Zaber VSR series stage (VSR40A-T3A) brings the sample into laser focus. Finally, the sample is transferred under the F-theta lens for laser ablation.

The depth of removal using the presented system is dependent on the used lasering parameters as well as the material that the laser is interacting with. The smallest achievable depth of removal with the presented system is below one micron for silicon.

2.3. LIBS signal collection system

The LIBS signal is collected using an Ocean Insight UV-grade optical fiber, along with a collimating lens having a focal length of approximately 5 mm. An optical setup is utilized during LIBS analysis to enhance the quality of the obtained signals. This setup comprises a dichroic beam splitter and two parabolic mirrors. The collected LIBS signal arrives at a parabolic mirror, which is utilized to collimate the divergent light. The collimated light then goes into a dichroic beam splitter, which reflects the light in the 240–840 nm wavelength range and passes through other wavelength values. This procedure filters out any unwanted background light and/or laser interference. The reflected light then arrives at a second parabolic mirror, which focuses the light onto the optical fiber, ensuring optimal signal detection. The Spectral Industries IRIS Echelle spectrometer disperses light into two perpendicular directions using two dispersive elements. Initially, the light passes through a prism that splits it into multiple orders, followed by a diffraction grating that separates the overlapping orders orthogonally. As a result, a sequence of various reflection orders is generated in a ladder-like arrangement on a complementary metal oxide semiconductor (CMOS) camera that has 1936 × 1216 pixels. The spectrometer has the capacity to measure wavelengths between 180 nm and 800 nm as well as between 880 nm and 1200 nm. Prior to measurements, a mercury Argon lamp is utilized to calibrate the spectrum. Fig. 3 schematically shows the described LIBS setup.

2.4. Signal processing and automated decision-making

Each material has its own characteristic peaks in the LIBS signal, which can be used to differentiate it from other materials. We used this

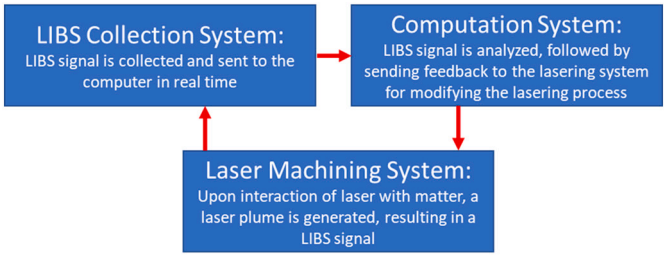

Fig. 1. Overview of the proposed system.

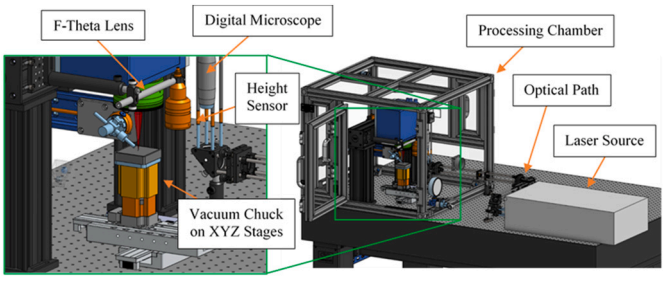

Fig. 2. CAD of femtosecond laser machining system.

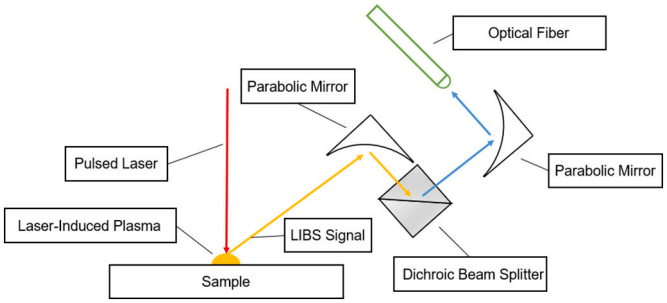

Fig. 3. LIBS setup.

to detect and discriminate different materials based on their characteristic peaks in the LIBS signal. The LIBS signals were collected during the laser ablation process of different materials. The collected signals were then analyzed to identify the characteristic peaks of each material. For each material of interest, frequency intervals containing the unique peaks were selected. As shown in Fig. 4, the peaks at 515.3 nm and 521.8 nm represent the characteristic peaks of copper, which were used to detect copper in the LIBS signals.

At the detection phase, each collected LIBS signal was analyzed to find out whether these intervals contain the characteristic peaks of the material. Our peak detection algorithm uses prominence as a criterion for identifying and selecting peaks of interest. By setting a prominence threshold, the algorithm could filter out smaller or less significant peaks, focusing only on those that meet the desired prominence criteria. If multiple peaks having prominences larger than the set threshold have been found, the peak with the largest prominence was selected as the detected characteristic peak. If a characteristic peak was found, the location being lasered was assigned to be that material.

In endpointing, some top layers need to be removed to expose the underlying layers for further processing. To achieve this, we need to avoid lasering certain materials. Therefore, as soon as the signal was detected to have the characteristic peak of the material of interest, the lasering process was stopped to preserve the layer containing that material. In this way, we can remove the top layers and stop at exactly the layer where the material of interest begins.

Depending on the application and the materials involved, one may choose to change the lasering parameters for different materials or stick to one set of parameters. The latter has been the case for the results shown in this paper. Having said that, the developed software algorithm allows for the automated changing of these parameters, based on the detected material. It is important to note that in many cases, adjusting the parameters based on the material that needs to be removed results in better performance in terms of quality and rate of removal.

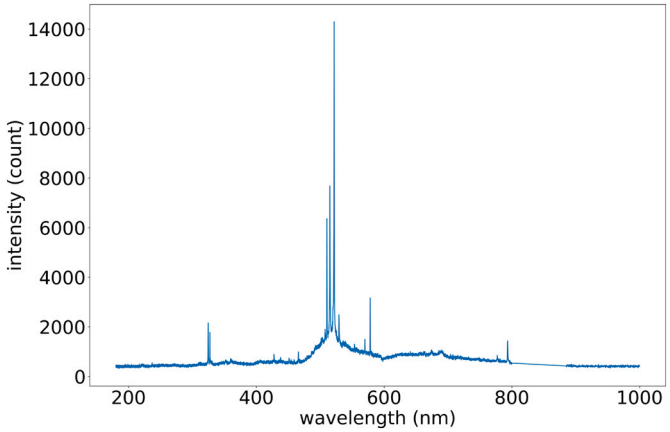

Fig. 4. Collected LIBS signal for copper.

2.5. Removal of dust and fume

The laser system is equipped with a vacuum exhaust system, which removes the created dust and fumes and filters them downstream. This addresses any health concerns in working with the described laser machining system.

3. Results and discussion

The capability of the proposed approach for vertical endpointing was demonstrated through multiple examples. The method used to generate the fs-LIBS signal in the majority of examples involves utilizing a burst of two pulses with a separation of 20 ns and a repetition rate of 10 kHz, while scanning the laser in a line pattern to create a trench at a speed of 1000 mm/s.

Each pulse has a fluence of 50 J/cm^2. The LIBS system camera is set to capture measurements at a frequency of 5 Hz with an exposure time of 50 ms. Fig. 5 schematically shows the Laser beam line pattern.

The study focuses on investigating four elements - Aluminium (Al), Silicon (Si), Copper (Cu), and an sn74ls08n integrated circuit.

The sample for the first example is a copper sheet, covered with aluminium foil, with a thickness of about 235 μm. Lasering from the top, where aluminium is present, the objective of the automated endpointing algorithm is to continue performing multiple cycles of lasering for material removal until copper is reached. Each lasering cycle removes about 2.5 μm of the aluminium material. Fig. 6 shows the color-coded confocal height map of the laser machining result, after the process is stopped by the automated endpointing algorithm. As can be inferred from the depth values, the process has stopped as soon as the complete thickness of the aluminium foil has been removed and copper has been reached.

The sample for the second example consists of a piece of thinned-down Si wafer on top of a copper sheet, where the thickness of the thinned-down Si wafer is ~135 μm. Similar to the first example, the objective is, starting from the top material, to continue performing laser machining cycles until the bottom material is reached. Each lasering cycle ablated ~1.5 μm of the Si material. Fig. 7 shows the color-coded confocal height map of the laser machining result, after the process is stopped by the automated endpointing algorithm. As can be inferred from the depth values, the process has stopped as soon as the complete thickness of the Si wafer has been removed and copper has been reached. The nonplanar regions, indicated by green color observed in the height map, correspond to copper regions that have been swelled due to suboptimal cutting parameters. In fact, the used cutting parameters are optimized for Silicon. This issue can be alleviated by working out lasering parameters that are optimized for both Si and Cu.

The sample for the third example is an sn74ls08n IC, with copper lead frame. The objective is, starting from an intact IC, to continue performing laser machining cycles to remove packaging material, until the copper lead frame is reached. Each lasering cycle ablated ~5 μm of packaging. Fig. 8 shows the color-coded confocal height map of the laser machining result, after the process is stopped by the automated endpointing algorithm. Fig. 9 shows an optical image of the lasered area. As can be seen in the images, the lasering process has stopped when the copper lead frame has been reached.

The sample for the fourth example is again a sn74ls08n IC. The

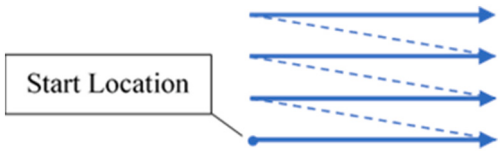

Fig. 5. Laser scanning pattern. The direction of the laser scan is indicated by the arrow, while the jump line is represented by the dotted line.

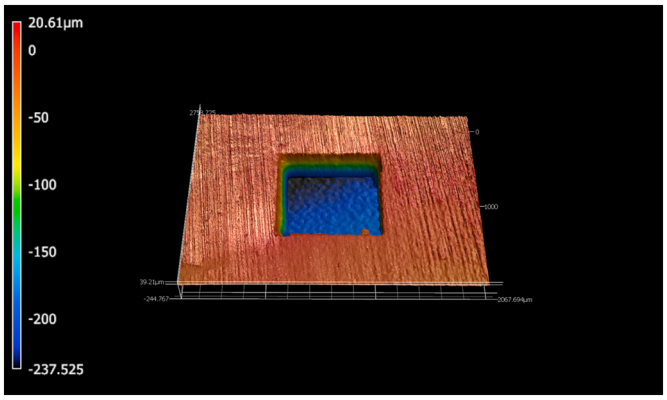

Fig. 6. Color-coded confocal height map of the laser machining result, for Al on Cu sample, after the process is stopped by the automated endpointing algorithm.

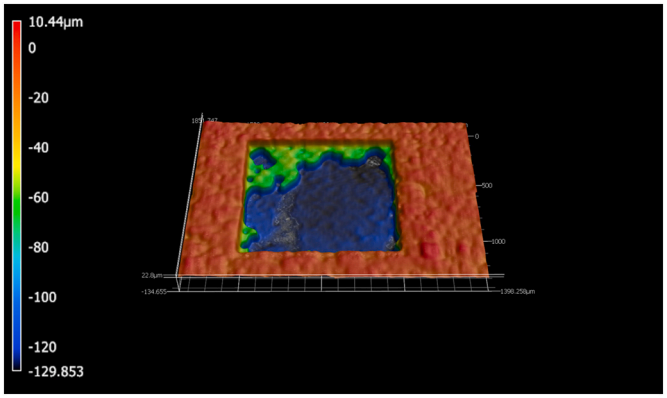

Fig. 7. Color-coded confocal height map of the laser machining result, for Si on Cu sample, after the process is stopped by the automated endpointing algorithm.

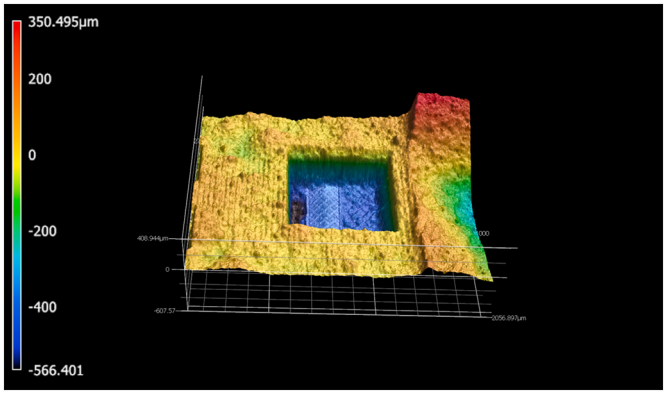

Fig. 8. Color-coded confocal height map of the laser machining result, for the IC sample with copper lead frame, after the process is stopped by the automated endpointing algorithm.

objective here is, starting from the back side of an intact IC, to continue performing laser machining cycles to remove packaging material as well as the lead frame until the silicon on the back side of the die is reached. The repetition rate has been adjusted to 100 kHz, and Each pulse has a fluence of 20 J/cm^2. Fig. 10 shows the progression of the machining process as well as the height map of the final surface profile when silicon is reached. Note that in the resulting surface, the entire backside of the

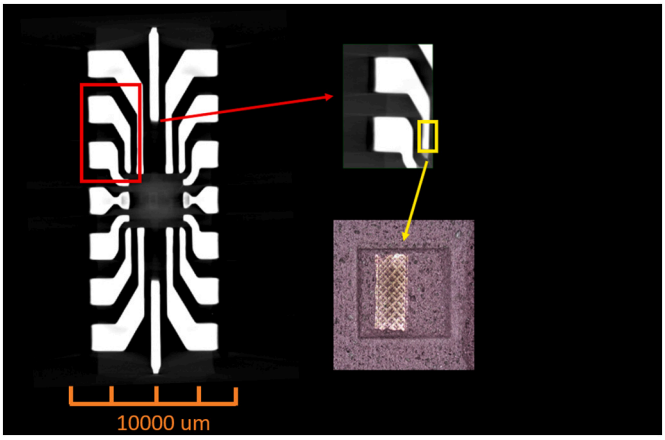

Fig. 9. Lead frame exposed after automated endpointing using the proposed algorithm.

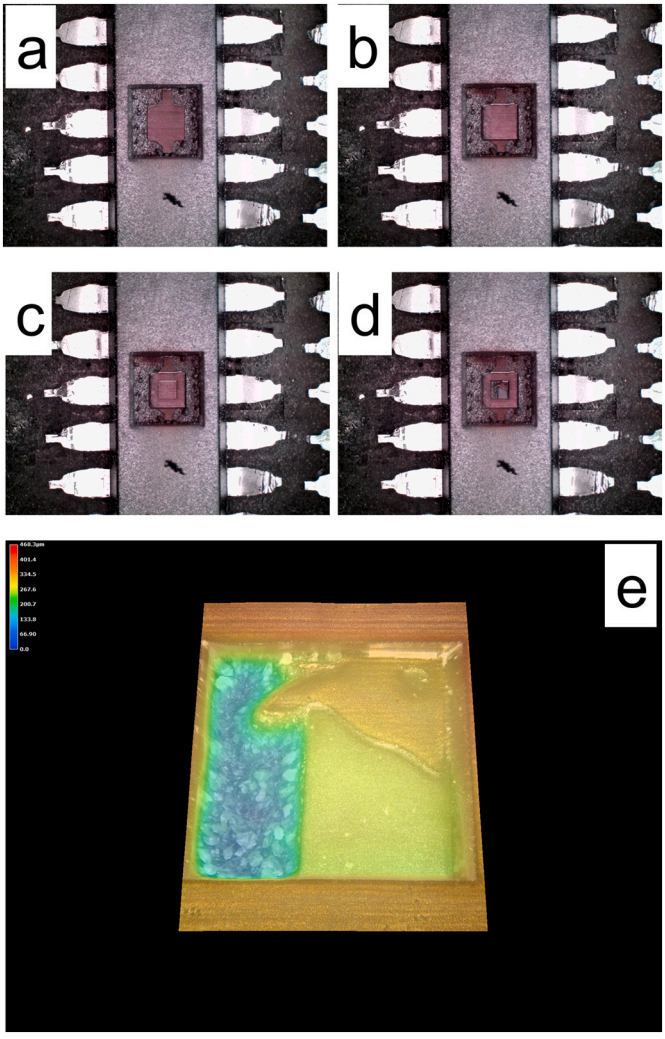

Fig. 10. (a) through (d): progression of the machining process with the objective of stopping at silicon on the backside of the die. Note that lasering area has been deliberately shrunk throughout the process to save on lasering time for the demonstration. Starting wide has been the case to enhance the gain of LIBS signal for highly accurate material detection; (e) height map of the final surface i.e. when silicon on the die backside is reached.

die has not been exposed upon detection of silicon which is due to the fact that the sample has been placed on the stage at a slightly unlevelled pose. This could be resolved in the future, in two ways: (1) the use of a tilt stage to compensate for any source of unlevelness, resulting in the backside being leveled with the horizon; and (2) the use of a variable-focusing laser scanning system to align the plane of focus with the unlevelled surface of the sample.

3.1. Use of proposed solution for industrial applications

This paper provides the proof-of-concept for the use of LIBS in tandem with ultrashort pulsed laser machining, for real-time material detection and endpointing. The current configuration of the proposed system offers great capabilities for lab-level sample preparation and failure analysis applications. Further, the modular aspect of the proposed machining system enables reconfiguration and customization of the tool to be used in any other industrial environment for various applications.

4. Scope and future direction

The proposed vertical endpointing solution provides the ability to stop at a certain layer if a certain material is present across the entire or only a portion of a layer of interest. An additional capability of the proposed LIBS solution is the ability to perform endpointing laterally, which is going to be among the future directions of the paper. For example, for the situation shown in Fig. 10, by implementing a parameter set that includes stopping the laser when it reaches the silicon, it would be possible to remove the packaging material without causing additional ablation to the exposed silicon.

The laser machining system, equipped with the LIBS data collection module, presented in this paper, is multi-purpose. It has the capability to perform device decapsulation, delayering, or targeted material removal for reaching the region of interest for follow-up failure analysis. As for the decapsulation purpose, the objective of the proposed solution is to improve the existing practice by negating the need for frequent visual checks on the device. Note that with a visual check approach, one should either pause the material removal process and investigate the top surface under an inspection microscope or camera for every layer that is being removed, which takes extensive time and manual effort, or should decrease the frequency of such inspections significantly to cut the required time and effort which significantly impacts the accuracy of the decapsulation procedure. With the proposed approach, the laser-delayering process stops automatically upon detection of the layer of interest, resulting in a procedure that does not or minimally requires manual effort while offering high degrees of precision.

5. Conclusion

This paper presents an automated vertical endpointing algorithm using LIBS, to be used in laser-enabled material processing. The presented method finds application in sample preparation and failure analysis of microelectronics. Several examples have been provided to showcase the capabilities of the proposed method. Further, the scope of applicability of the proposed solution goes beyond the test cases showcased herein. Particularly, the proposed solution facilitates rapid, high-precision, automated material processing for verification and validation as well as fabrication in 3D heterogeneous integration (3DHI) applications, towards assurance and improved yields.

CRediT authorship contribution statement

All authors contributed to conceptualization, data curation, formal analysis, investigation, methodology, visualization, and writing. Additionally, corresponding authors contributed to project administration and supervision.

Declaration of competing interest

The authors declare that they have no known competing financial interests or personal relationships that could have appeared to influence the work reported in this paper.

Data availability

Data is provided in the paper

References

[1] Ping Li, et al., Recent advances in focused ion beam nanofabrication for nanostructures and devices: fundamentals and applications, Nanoscale 13 (3) (2021) 1529–1565.
[2] Karen Sloyan, et al., A review of focused ion beam applications in optical fibers, Nanotechnology 32 (47) (2021), 472004.
[3] Jinqiao Liu, et al., Effect of ion irradiation introduced by focused ion-beam milling on the mechanical behaviour of sub-micron-sized samples, Sci. Rep. 10 (1) (2020) 1–8.
[4] Grzegorz Greczynski, Lars Hultman, X-ray photoelectron spectroscopy: towards reliable binding energy referencing, Prog. Mater. Sci. 107 (2020), 100591.
[5] Thomas R. Gengenbach, et al., Practical guides for x-ray photoelectron spectroscopy (XPS): interpreting the carbon 1s spectrum, J. Vac. Sci. Technol. A 39 (1) (2021), 013204.
[6] Fred A. Stevie, Carrie L. Donley, Introduction to x-ray photoelectron spectroscopy, J. Vac. Sci. Technol. A 38 (6) (2020), 063204.
[9] Ying Wang, et al., Study of signal enhancement in collinear femtosecond-nanosecond double-pulse laser-induced breakdown spectroscopy, Opt. Laser Technol. 122 (2020), 105887.
[10] Ying Wang, et al., Enhanced optical emission in laser-induced breakdown spectroscopy by combining femtosecond and nanosecond laser pulses, Phys. Plasmas 27 (2) (2020), 023507.
[11] Johannes D. Pedarnig, et al., Review of element analysis of industrial materials by in-line laser—induced breakdown spectroscopy (LIBS), Appl. Sci. 11 (19) (2021) 9274.
[12] Yanwei Yang, et al., Application of scikit and keras libraries for the classification of iron ore data acquired by laser-induced breakdown spectroscopy (LIBS), Sensors 20 (5) (2020) 1393.
[13] Adrian Phoulady, et al., A novel material detection method using femtosecond laser, confocal imaging and image processing enabling endpointing in fast inspection of microelectronics, Microelectron. Reliab. 126 (2021), 114287.
[14] Nicholas May, et al., Correlative multimodal imaging and targeted lasering for automated high-precision IC decapsulation, Microelectron. Reliab. 138 (2022), 114660.
[15] N. May, H. Choi, A. Phoulady, S. Amini, P. Tavousi, S. Shahbazmohamadi, Gas-assisted femtosecond pulsed laser machining: a high-throughput alternative to focused ion beam for creating large, high-resolution cross sections, PLoS One 18 (5) (2023), e0285158.
[16] M. Konnik, B. Ahmadi, N. May, J. Favata, Z. Shahbazi, S. Shahbazmohamadi, P. Tavousi, Training AI-based feature extraction algorithms, for micro CT images, using synthesized data, J. Nondestr. Eval. 40 (2021 Mar) 1–3.
[17] A. Phoulady, N. May, H. Choi, Y. Suleiman, S. Shahbazmohamadi, P. Tavousi, Rapid high-resolution volumetric imaging via laser ablation delayering and confocal imaging, Sci. Rep. 12 (1) (2022 Jul 19) 12277.
[18] H. Choi, N. May, A. Phoulady, Y. Suleiman, D. DiMase, S. Shahbazmohamadi, P. Tavousi, Rapid three-dimensional reconstruction of printed circuit board using femtosecond laser delayering and digital microscopy, Microelectron. Reliab. 138 (2022 Nov 1) 114659.
[19] N. May, H. Choi, A. Phoulady, Y. Suleiman, D. DiMase, P. Tavousi, S. Shahbazmohamadi, Correlative multimodal imaging and targeted lasering for automated high-precision IC decapsulation, Microelectron. Reliab. 138 (2022 Nov 1) 114660.
[20] P. Hoveida, A. Phoulady, H. Choi, N. May, Shahbazmohamadi S, Tavousi P. Terahertz-readable laser engraved marks as a novel solution for product traceability, Sci. Rep. 13 (1) (2023 Aug 1) 12474.